Progress In Electromagnetics Research, PIER 24, 119–138, 1999

EFFECTIVE PERMITTIVITY OF DRY SNOW IN THE 18 TO 90 GHz RANGE

W. Huining, J. Pulliainen, and M. Hallikainen

Helsinki University of Technology
Laboratory of Space Technology
P.O. Box 3000
FIN-02015, Finland

1. INTRODUCTION

In remote sensing modeling, natural media such as dry snow can be characterized by the effective permittivity. It determines the behavior of electromagnetic wave including wave propagation, attenuation, scattering and emission.

Effective permittivity models have been studied extensively. Among those models, empirical and theoretical mixing models for dry snow include the Hallikainen model [1] and Mätzler model [2] for the real part of the dielectric constant, and the Tiuri model [3], PVS model and Tinga model [1] for the dielectric loss factor. These models are limited to the low-frequency approximation for which the effects of scattering are neglected. This limitation means that the dielectric constant is not dependent on snow grain size. In order to investigate the dielectric properties of snow at higher frequencies, the strong fluctuation theory is used to derive the expression of the effective permittivity [4]–[9], in which the effect of scattering between ice particles is taken into account. In the strong fluctuation theory, dry snow is described by a correlation function. A spherical symmetric correlation function is used in this paper.

Presently, experimental effective permittivity values of snow are available for a limited frequency range. The real part of the effective permittivity ε'_{eff} is known for frequencies up to 37 GHz and the imaginary part of effective permittivity ε''_{eff} for frequencies up to 13 GHz [1]. It is very difficult to measure the imaginary part of effective permittivity of snow at high frequencies. One possibility is the use of radiometric techniques. Using radiometric techniques, and by eliminating the effect of scattering, the imaginary part of effective permittivity ε''_{eff} was measured up to 94 GHz for two snow densities [10]. In the case of homogeneous media (such as pure ice), the determination of the imaginary part of the effective permittivity in 10 to 100 GHz range is accurate by using radiometric techniques [11]. However, dry snow is an inhomogeneous medium. The scattering effect by ice particles cannot be neglected. Thus, the values based on the radiometric techniques are not accurate at high frequencies for dry snow.

In this paper, experimental data of extinction coefficients of dry snow in the 18 to 90 GHz range [10] are employed to derive the empirical values of effective permittivity. The range of the validity of strong fluctuation theory model for the dry snow effective permittivity is examined by comparing the model predictions with experimental data-based values.

2. THE EMPIRICAL VALUES OF EFFECTIVE PERMITTIVITY

Dry snow is a mixture of ice particles and air. The underlying concept of effective permittivity (ε_{eff}) of dry snow is that the coherent (average) scattered field from an inhomogeneous dry snow pack should be equal to the field scattered from a corresponding homogeneous medium with permittivity ε_{eff} [12]. The behavior of the electromagnetic wave in dry snow is determined by the effective permittivity. The effective permittivity of dry snow is a function of size, shape, complex permittivity and volume fraction of ice particles. In this paper, spherical shape for ice particles is assumed.

It is difficult to measure the imaginary part of the effective permittivity of dry snow at high frequencies by using ordinary measurement techniques. In this section, the experimental data on extinction coefficients κ_e of dry snow in the 18 to 90 GHz range are employed to derive the empirical values of effective permittivity.

In the radiative transfer theory, the total loss of dry snow is expressed by the extinction coefficient κ_e, which includes both absorption loss and scattering loss.

$$\kappa_e = \kappa_a + \kappa_s \quad , \tag{1}$$

where the absorption coefficient κ_a represents the absorption loss and the scattering coefficient κ_s represents the scattering loss.

The extinction coefficient κ_e is related to the effective permittivity ε_{eff} via the equation [10]:

$$\kappa_e = 2k_0 \mathrm{Im}\left|\sqrt{\varepsilon_{eff}}\right| \tag{2}$$

where k_0 is the free-space propagation constant. The expression in (2) is analogous to that for the absorption coefficient

$$\kappa_a = 2k_0 \mathrm{Im}\left|\sqrt{\varepsilon_g}\right| \tag{3}$$

where ε_g is the quasi-static value of the dielectric constant.

The complex effective permittivity in (2) can be written as $\varepsilon_{eff} = \varepsilon'_{eff} - i\varepsilon''_{eff}$. Calculation of the imaginary part of effective permittivity ε''_{eff} from (2) requires knowledge of the real part of effective permittivity ε'_{eff}. Fortunately, recent experimental and numerical analysis

have shown that a simple low-frequency mixing formula can accurately predict the real part of effective permittivity ε'_{eff} of random media at high frequencies [13]. In this paper, the PVS model [1] is used to calculate the real part of effective permittivity ε'_{eff}. Equation (2) can be solved by numerical method. For materials with $\varepsilon'_{eff}/\varepsilon''_{eff} < 0.1$, ε''_{eff} can be approximated by:

$$\varepsilon''_{eff} = \frac{\kappa_e \sqrt{\varepsilon'_{eff}}}{k_0} \tag{4}$$

The experimental data on the extinction coefficient are adopted from Hallikainen et al.'s paper [10]. In that paper, the extinction coefficients for several snow types were obtained from transmission-loss measurements of snow slabs as a function of sample thickness. The effect of frequency, mean grain size, density and temperature of dry snow were investigated in a detailed manner. In the derivation of the approximate expression for the extinction coefficient, it was assumed that the scattering is concentrated in the forward direction.

3. THE EFFECTIVE PERMITTIVITY MODELS FOR DRY SNOW

3.1 Empirical and Theoretical Mixing Models for Dry Snow Dielectric Constant

Real part of the dielectric constant of dry snow ε'_{ds} is independent on temperature and frequency. It is found that ε'_{ds} is a function of the dry snow density ρ_{ds} only, and the suggested empirical and theoretical mixing models are [1], [2]:

$$\begin{cases} \varepsilon'_{ds} = 1 + 1.83\rho_{ds} & \rho_{ds} \le 0.5 g/cm^3 \\ \varepsilon'_{ds} = 0.51 + 2.88\rho_{ds} & \rho_{ds} \ge 0.5 g/cm^3 \end{cases} \qquad \text{Hallikainen model} \tag{5}$$

$$\varepsilon'_{ds} = 1 + \frac{1.58\rho_{ds}}{1 - 0.365\rho_{ds}} \qquad \text{Mätzler model} \tag{6}$$

where ρ_{ds} is the dry snow density in g/cm^3.

The dielectric loss factor of dry snow is dependent on density, temperature, frequency, grain size and other parameters, such as acidity.

The empirical and theoretical mixing models for dry snow are limited to the low-frequency approximation for which the effects of scattering were neglected. This limitation means that the dielectric constant is not dependent on grain size. Several empirical and theoretical mixing models for dielectric loss factor have been suggested [1], [3]:

$$\varepsilon''_{ds} = \varepsilon''_{ice}(0.52\rho_{ds} + 0.62\rho^2_{ds}) \qquad \text{Tiuri model} \qquad (7)$$

$$\varepsilon''_{ds} = 3\varepsilon''_{ice} f_\nu \frac{(\varepsilon'_{ds})^2(2\varepsilon'_{ds}+1)}{(\varepsilon'_{ice}+2\varepsilon'_{ds})\left[\varepsilon'_{ds}+2(\varepsilon'_{ds})^2\right]} \qquad \text{PVS model} \qquad (8)$$

$$\varepsilon''_{ds} = \frac{9 f_\nu \varepsilon''_{ice}}{\left[(2+f_\nu)+\varepsilon''_{ice}(1-f_\nu)\right]^2} \qquad \text{Tinga model} \qquad (9)$$

where $\varepsilon_{ice} = \varepsilon'_{ice} - i\varepsilon''_{ice}$ is the relative complex permittivity of ice, $f_\nu = \rho_{ds}/\rho_{ice}$ is the ice fraction volume, and $\rho_{ice} = 0.916\ g/cm^3$ is the density of ice. At microwave frequencies ($10\ MHz$ - $100\ GHz$), the real part of the ice permittivity may be considered independent of both temperature and frequency, and may be assigned the constant value $\varepsilon'_{ice} = 3.15$ [10, 14]. The imaginary part of the ice permittivity ε''_{ice} is a function of frequency, temperature and impurity. Formulas for ε''_{ice} can be found in [15] for pure ice and in [11] for impure ice.

3.2 Strong Fluctuation Models for Dry Snow Dielectric Constant

Consider a continuous random medium in which scatterers with permittivity ε_s are embedded in a background medium with permittivity ε_b. The fraction volume occupied by the scatterers is f_ν and the fraction volume occupied by the background medium is $1 - f_\nu$. For the case of snow, the scatterers are ice particles and the background is air. The permittivity of scatterers is $\varepsilon_s = \varepsilon_{ice}$ and the permittivity of background is $\varepsilon_b = \varepsilon_{air} = 1$.

In the low frequency limit, the effective permittivity of snow under the bilocal approximation in the strong fluctuation theory for spherically symmetric correlation function is [4]:

$$\varepsilon_{eff} = \varepsilon_g + i\frac{2}{3}\delta k_0^2 k_g \varepsilon_0 \int_0^\infty dr\ r^2\ ACF(r) \qquad (10)$$

where ε_g (the quasi-static dielectric constant) is the solution of the

non-linear equation [6]

$$f_\nu \left(\frac{\varepsilon_s - \varepsilon_g}{\varepsilon_s + 2\varepsilon_g} \right) + (1 - f_\nu) \cdot \left(\frac{\varepsilon_b - \varepsilon_g}{\varepsilon_b + 2\varepsilon_g} \right) = 0 \tag{11}$$

The variance of the fluctuation δ in (10) is [6]:

$$\delta = 9\frac{\varepsilon_g^2}{\varepsilon_0^2} \left[f_\nu \left(\frac{\varepsilon_s - \varepsilon_g}{\varepsilon_s + 2\varepsilon_g} \right)^2 + (1 - f_\nu) \cdot \left(\frac{\varepsilon_b - \varepsilon_g}{\varepsilon_b + \varepsilon_g} \right)^2 \right] \tag{12}$$

In (10), $k_0 = \omega\sqrt{\varepsilon_0 \mu_0}$ is the wave number of free space. The wave number $k_g = \omega\sqrt{\varepsilon_g \mu_0}$.

$ACF(r)$ in (10) is the autocorrelation function. If the correlation function is selected as: $ACF(r) = \exp(-r/L)$, where L is the correlation length, we have

$$\varepsilon_{eff,L} = \varepsilon_g + i\frac{4}{3}\delta k_0^2 k_g \varepsilon_0 \cdot L^3 \tag{13}$$

We call (13) the low-frequency model for permittivity.

Dielectric constant formulations for general cases with an exponential correlation function are given in [5].

$$\varepsilon_{eff,G} = \varepsilon_g + k_0^2 \delta \left(\frac{2I_1}{3} - \frac{iI_2}{k_g} - \frac{I_3}{3} + \frac{I_4}{k_0^2 \varepsilon_g} \right) \tag{14}$$

where

$$I_1 = \frac{I}{\beta^2 + k_g^2} \tag{15}$$

$$I_2 = -\frac{3\beta}{2k_g^2} + \frac{1}{2k_g} \left(\frac{3\beta^2}{k_g^2} + 1 \right) \tan^{-1} \frac{k_g}{\beta} \tag{16}$$

$$I_3 = \frac{3}{k_g^2} - \frac{1}{\beta^2 + k_g^2} - \frac{3\beta}{k_g^3} \tan^{-1} \frac{k_g}{\beta} \tag{17}$$

$$I_4 = \frac{1}{3} - \frac{\beta^2}{2k_g^2} - \frac{\beta}{2k_g} \left(\frac{\beta^2}{k_g^2} + 1 \right) \tan^{-1} \frac{k_g}{\beta} \tag{18}$$

with

$$\beta = \frac{1}{L} - ik_g \tag{19}$$

where L is correlation length. We call (14) the general model for permittivity. The difference between (13) and (14) was discussed in detail in [5].

The numerical results show that at low frequencies (below $18\,GHz$), the differences between prediction from (13) and (14) are very small. At high frequencies, Equation (13) always overestimates the imaginary part of dielectric constant (see Section IV).

4. RESULTS

In the following calculation, pure ice permittivity is used [15], and ACF are of an exponential form $ACF(r) = \exp(-r/L)$.

4.1 Comparison of the Empirical and Theoretical Mixing Models for Dry Snow with the Quasi Static Permittivity ε_g of Strong Fluctuation Theory

At low-frequency approximation for which the effects of scattering were neglected, we have:

$$\varepsilon_{eff} \approx \varepsilon_g \tag{20}$$

Now we compare empirical and theoretical mixing models for the dry snow permittivity with the quasi static permittivity ε_g in the strong fluctuation theory. The frequency is $f = 9.375GHz$.

The comparison of real part of ε_g with Hallikainen model given in (5) and Mätzler model given in (6) are shown in Figure 1. The difference between the values predicted by these models is marginal.

The imaginary part of ε_g was compared with the imaginary part predicted by the Tiuri model (7), PVS model (8) and Tinga model (9) by analyzing the ratio of the modeled dielectric loss factor of dry snow ε''_{ds} to the ice loss factor ε''_{ice}:

$$\Delta\varepsilon'' = \frac{\varepsilon''_{ds}}{\varepsilon''_{ice}} \tag{21}$$

Figure 2 shows that the imaginary part of ε_g is identical to the PVS model. Actually, at frequencies below the low-frequency limit, ε_g according to the strong fluctuation theory (11) is identical to the PVS model given by (8). Tsang et al. [4] also obtained the same conclusion.

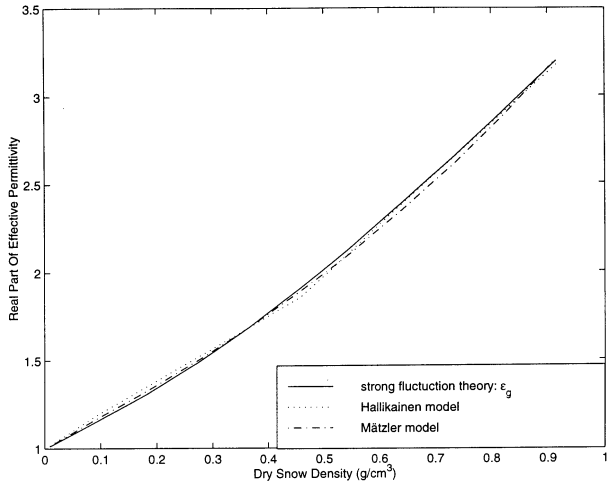

Figure 1. Comparison of real part of ε_g with dry snow dielectric models

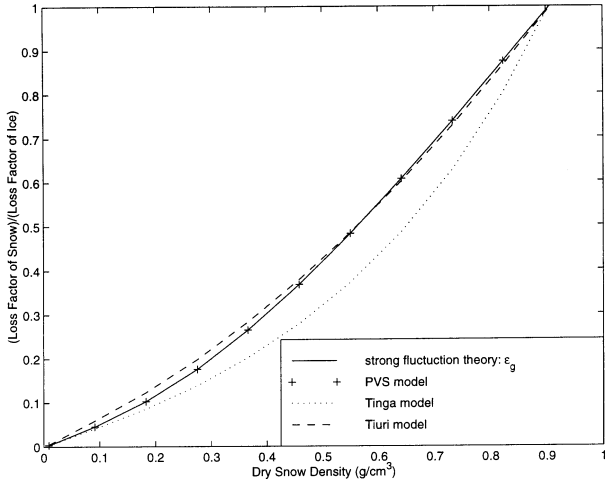

Figure 2. Comparison of the ratio of snow loss factor to ice loss factor using the quasi-static permittivity of snow ε_g and dry snow dielectric models.

4.2 The Properties of Effective Permittivity Models of Snow in Strong Fluctuation Theory

We now calculate the effective permittivity of snow ε_{eff} using the low-frequency model (13) denoted by $\varepsilon_{eff,L}$ and general model (14) denoted by $\varepsilon_{eff,G}$ and compare them with the quasi static permittivity ε_g.

4.2.1 Permittivity as a Function of Dry Snow Density

First, we calculate the permittivity as a function of dry snow density. The frequency is $10.0\ GHz$. The real part of the permittivity $\varepsilon_{eff,L}$, $\varepsilon_{eff,G}$ and ε_g as a function of dry snow density is shown in Figure 3(a). The results show that there is no difference between the real part of $\varepsilon_{eff,L}$, $\varepsilon_{eff,G}$ and ε_g. However, in the case of the imaginary part of the permittivity, a small difference exists. This can be seen in Figure 3(b) which shows the ratio of the snow loss factor to the ice loss factor for the two ε_{eff} models and for ε_g. The results are depicted for different correlation lengths at $L = 0.15\ mm$, $L = 0.3\ mm$ and $L = 0.45\ mm$. Figure 3(b) shows that the imaginary part of the permittivity ε_{eff} is dependent on the correlation length and it is always larger than that of ε_g. An interesting aspect is that when the correlation length is equal to $0.45mm$ and the snow density is equal to 0.4, the imaginary part of ε_{eff} exceeds the imaginary part of ε_{ice}, $\mathrm{Im}(\varepsilon_{eff})/\mathrm{Im}(\varepsilon_{ice}) > 1$. The maximum value is obtained when the snow density equals to 0.7. This phenomenon is caused by the effect of scattering. When the fraction volume is equal to 1, the ratio $\mathrm{Im}(\varepsilon_{eff})/\mathrm{Im}(\varepsilon_{ice}) = 1$. This is a reasonable result because the fraction volume equal to 1 means that the material is ice.

Next, we examine the permittivity behavior at a high frequency, $f = 35\ GHz$. The real part of the permittivity $\varepsilon_{eff,L}$, $\varepsilon_{eff,G}$ and ε_g as a function of dry snow density at $f = 35\ GHz$ are shown in Figure 4(a).

Figure 4(a) shows that there is no difference between $\varepsilon_{eff,L}$ and ε_g. For the general model, the real part of the permittivity $\varepsilon_{eff,G}$ slightly deviates from ε_g. It shows values of $\varepsilon_{eff,G}$ always larger than ε_g. In the calculation, three correlation lengths are used. This is shown in the figure using three circles at each density for $\varepsilon_{eff,G}$.

The ratio of the imaginary part of the permittivity $\varepsilon_{eff,L}$, $\varepsilon_{eff,G}$ and ε_g of snow to the ice loss factor as a function of dry snow density

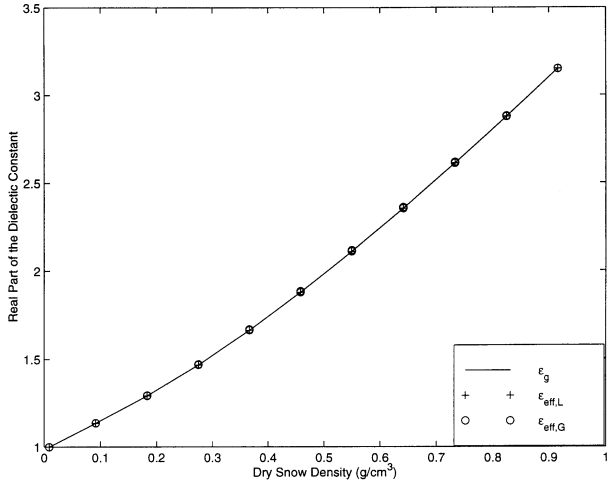

(a)

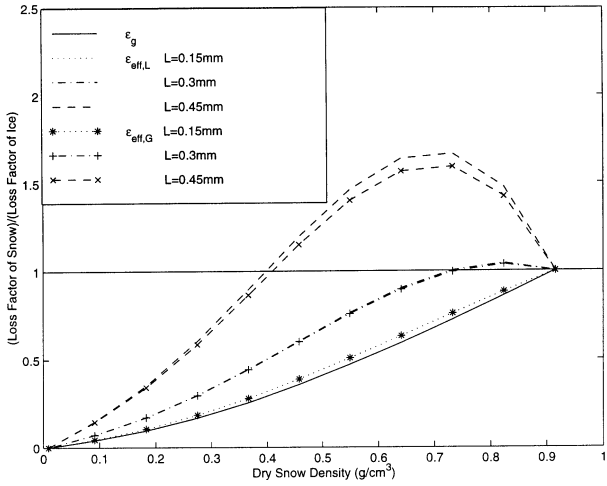

(b)

Figure 3. (a) Comparison of real part of ε_g with ε_{eff} as a function of dry snow density at $f = 10\ GHz$; (b) Comparison of the ratio of snow loss factor to ice loss factor using the two ε_{eff} models and ε_g as a function of dry snow density at $f = 10\ GHz$.

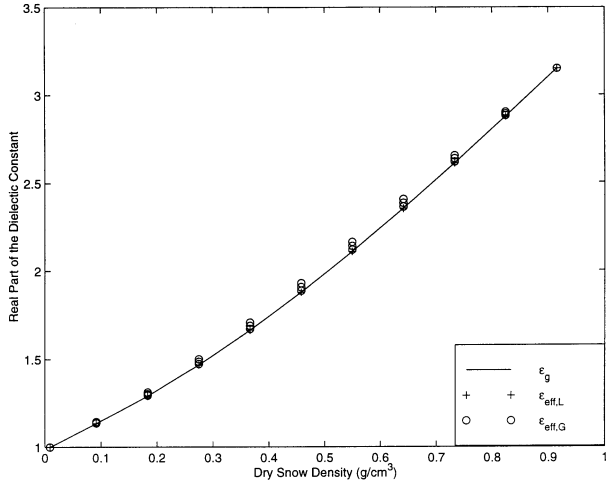

(a)

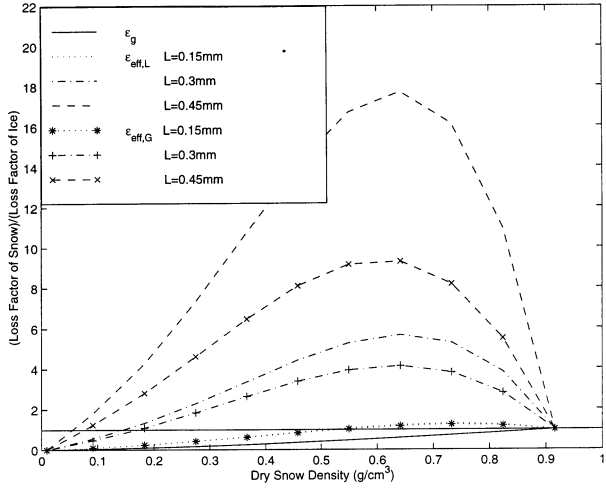

(b)

Figure 4. (a) Comparison of real part of ε_g with ε_{eff} as a function of dry snow density at $f = 35\ GHz$; (b) Comparison of the ratio of snow loss factor to ice loss factor using the two ε_{eff} models and ε_g as a function of dry snow density at $f = 35\ GHz$.

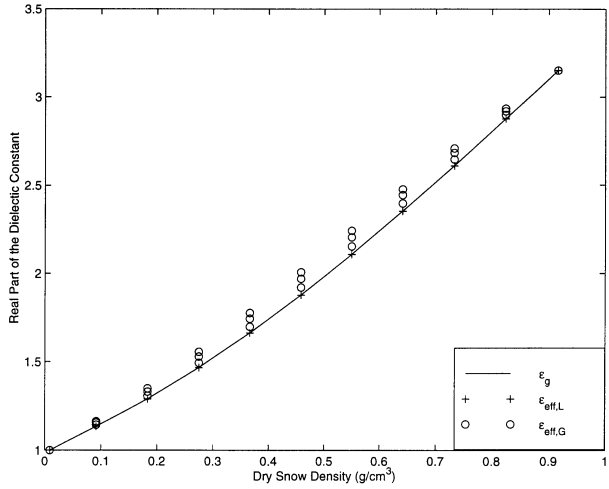

(a)

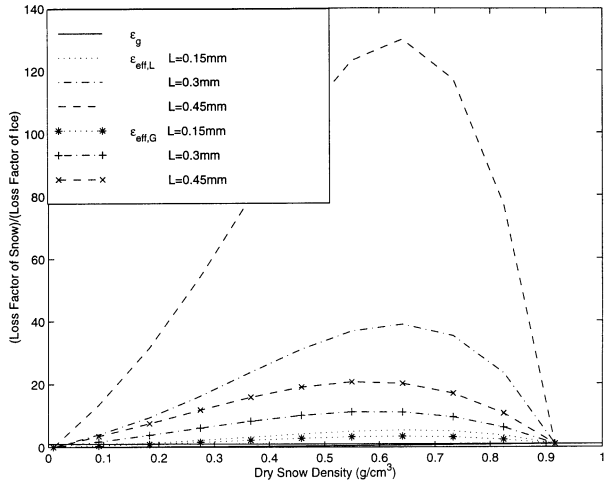

(b)

Figure 5. (a) Comparison of real part of ε_g with ε_{eff} as a function of dry snow density at $f = 90\ GHz$; (b) Comparison of the ratio of snow loss factor to ice loss factor using the two ε_{eff} models and ε_g as a function of dry snow density at $f = 90\ GHz$.

at $f = 35\ GHz$ is shown in Figure 4(b). The results are depicted for different correlation lengths at $L = 0.15\ mm$, $L = 0.3\ mm$ and $L = 0.45\ mm$.

We note that there is only a small difference between the low-frequency model and the general model at a small correlation length ($L = 0.15\ mm$). For a large correlation length ($L = 0.3\ mm$ and $L = 0.45\ mm$), the difference between the low-frequency model and general model is very large. Therefore, the low-frequency model is not valid for high frequencies.

The real part of the permittivity $\varepsilon_{eff,L}$, $\varepsilon_{eff,G}$ and ε_g as a function of dry snow density at $f = 90\ GHz$ are shown in Figure 5(a). Again, we can see from Figure 5(a) that there is no difference between $\varepsilon_{eff,L}$ and ε_g and a moderate difference between $\varepsilon_{eff,G}$ and ε_g.

The ratio of the imaginary part of the permittivity $\varepsilon_{eff,L}$, $\varepsilon_{eff,G}$ and ε_g of snow to ice loss factor as a function of dry snow density at $f = 90\ GHz$ are shown in Figure 5(b). The results are depicted for different correlation lengths at $L = 0.15\ mm$, $L = 0.3\ mm$ and $L = 0.45\ mm$. The results indicate that the values of the imaginary part of $\varepsilon_{eff,L}$, $\varepsilon_{eff,G}$ are too high at $90\ GHz$, especially for the imaginary part of $\varepsilon_{eff,L}$.

4.2.2 Permittivity as a Function of Frequency

Secondly, we calculate the permittivity as a function of frequency. The fraction volume is selected to be $f_\nu = 0.4$.

The real part of the permittivity $\varepsilon_{eff,L}$, $\varepsilon_{eff,G}$ and ε_g as a function of frequency is shown in Figure 6(a). Figure 6(a) indicates that there are only small differences between $\varepsilon_{eff,L}$ and ε_g when $f > 40\ GHz$. The differences increase as the correlation lengths increase. As the frequency or the correlation length increases, the real part of $\varepsilon_{eff,L}$ tends to slightly decrease. On the other hand, the real part of $\varepsilon_{eff,G}$ increases as the frequency and/or correlation lengths increase.

The ratio of the loss factor of snow according to permittivities $\varepsilon_{eff,L}$, $\varepsilon_{eff,G}$ and ε_g to the loss factor of ice as a function of frequency is shown in Figure 6(b). The results are depicted for different correlation lengths. Figure 6(b) shows that the imaginary parts of the permittivity ε_{eff} is dependent on the frequency and on the correlation lengths and that it is always larger than that of ε_g. At low frequency limit(below $18\ GHz$), the difference between the low frequency model and the general model is very small. The difference between these two

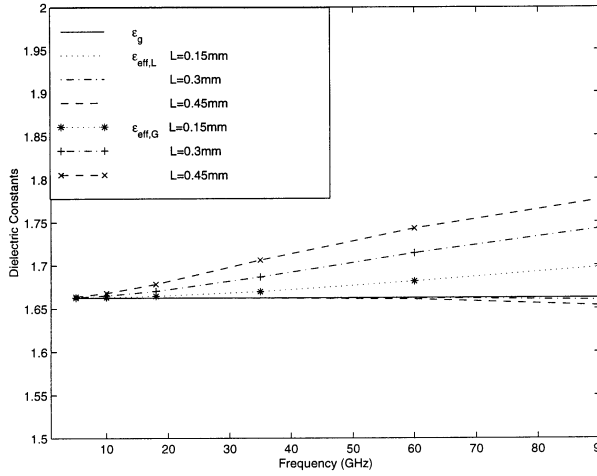

(a)

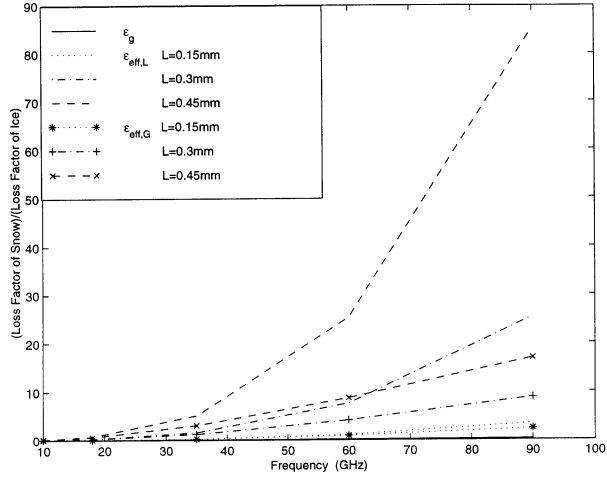

(b)

Figure 6. (a) Comparison of real part of ε_g with ε_{eff} as a function of frequency; (b) Comparison of the ratio of snow loss factor to ice loss factor as a function of frequency using the two ε_{eff} models and ε_g.

models increases when the frequency and correlation lengths increases. At high frequencies, the low-frequency model always overestimates the imaginary part of the dielectric constant. We also note that the imaginary part of ε_{eff} increases faster than that of ε_{ice} at high frequencies.

4.3 Comparison of the Model Predictions with the Experimental Data-based Values

According to [10], the snow extinction coefficient can be determined by measuring the transmission-loss factor $L(dB)$ as a function of the snow slab thickness. In [10], the transmission loss for 18 snow samples was measured at 18, 35, 60 and 90 GHz using a free-space transmission experiment system. During the measurements, the samples were handled and stored at $-15°C$. The properties of 18 snow samples and the experimental extinction coefficient κ_e for 18 snow samples can be found in [10]. For easy reference, the properties of 18 snow samples are listed in Table 1.

No.	Date	Depth in snowpack	Observed mean grain size (mm)	Surface roughness (mm)	Density g / cm^3	Dielectric constant at 10 GHz	Comments
1	Feb. 1	Top	0.2	0	0.172	1.31	One-hour old snow
2	Feb.15	Near Top	0.5	0	0.194	1.34	Newly fallen snow
3	Feb.16	Near Top	0.7	0	0.217	1.39	Newly fallen snow
4	Feb.18	Top	0.2	0	0.322	1.58	5-day old snow
5	Mar.12	Top	0.3	0	0.277	1.52	
6	Mar.12	Middle	0.9	0	0.268	1.49	Separate grains
7	Mar.18	Near Top	0.4	0	0.235	1.41	Newly fallen snow
8	Mar.21	Near Bottom	1.0	1	0.315	1.58	
9	Mar.29	Top	1.0	1	0.385	1.75	Hard snow
10	Mar.29	Near Bottom	1..0	1	0.276	1.50	Separate grains
11	Apr. 7	Top	1.3	2 to 3	0.307	1.61	
12	Apr.11	Top	1.2	3	0.304	1.61	
13	Apr.11	Near Bottom	1.3	1 to 3	0.293	1.54	
14	Apr.13	Top	1.5	2 to 3	0.345	1.64	
15	Apr.13	Middle	1.1	1 to 2	0.332	1.63	
16	Apr.16	Bottom	1.1	1 to 2	0.361	1.77	Separate grains
17	Apr.17	Top	1.5	2 to 4	0.390	1.79	
18	Apr.30	Near Top	1.6	2 to 3	0.351	1.66	

Table 1. Properties of 18 snow samples.

Using Equation (2), the imaginary part of $\varepsilon_{eff,L}$ for 18 snow samples at 18, 35, 60 and 90 GHz were calculated. The effective permittivity $\varepsilon_{eff,G}$ for 18 snow samples at 18, 35, 60 and 90 GHz are also calculated by using the strong fluctuation model (14). In order to compare the values obtained by using (14) with those estimated using (2), the relationship between the grain radius and the correlation length is selected to be [16]

$$L = \frac{4}{3}a \tag{22}$$

where L is the correlation length and a is the mean grain radius. A comparison of theoretical values according to (14) and experimental results according to (2) is shown in Figure 7. The comparison indicates that the results of the strong fluctuation model for effective permittivity fit the experimentally determined effective permittivity at $35\ GHz$ and $60\ GHz$. The strong fluctuation model-based values are substantially smaller than the experimental effective permittivities at $18\ GHz$. However, in this case the experimental values of the effective permittivity may be biased due to the low transmission loss at $18\ GHz$ (mostly below 1 dB even for thick snow samples) [10]. At $90\ GHz$, the model predictions fit well the experimental effective permittivity for grain sizes smaller than $0.9\ mm$ (samples 1–8). For grain sizes larger than $0.9\ mm$ the model-derived values are higher than the experimental effective permittivities (samples 9–18).

Thus, we can say that the strong fluctuation theory provides reasonable accurate results for the effective permittivity in the 1- to 100-GHz range except for large grain sizes at high frequencies $(60 \sim 90\ GHz)$.

5. CONCLUSION

In this paper, the empirical values of effective permittivity of dry snow in the 18-90 GHz range are derived from the experimental data on the extinction coefficient of dry snow. The range of validity of strong fluctuation theory models and several empirical and theoretical mixing models for dry snow effective permittivity are examined by comparing the model predictions with empirical values. Recent experimental and numerical analysis have shown that a simple low-frequency mixing formula can accurately predict the real part of effective permittivity ε'_{eff} of random media at high frequencies [13]. In this paper, it is shown that the strong fluctuation theory model of Stogryn [5] provides reasonable accurate results for the imaginary part of the effective per-

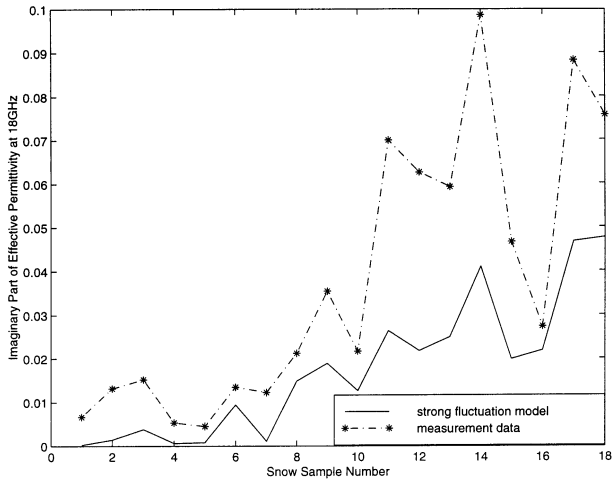

(a)

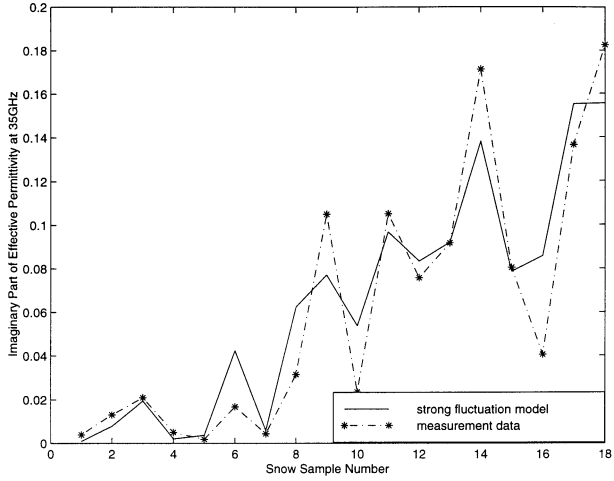

(b)

Figure 7. The imaginary part of effective permittivity of 18 snow samples at (a) 18 *GHz*, (b) 35 *GHz*. Note that the imaginary part of effective permittivity is a function of mean radius of ice particles, dry snow density and temperature of snow samples. These characteristics of the employed 18 snow samples are given in Table 1.

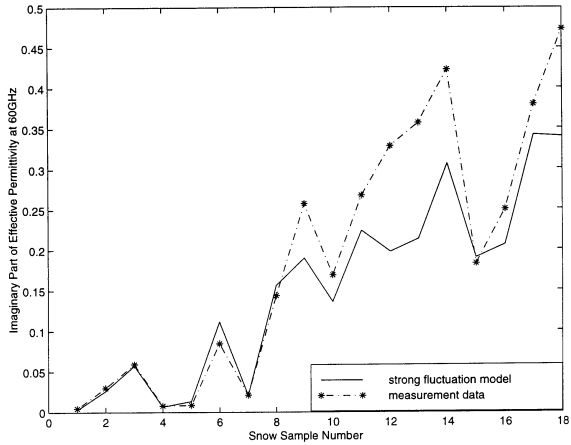

(c)

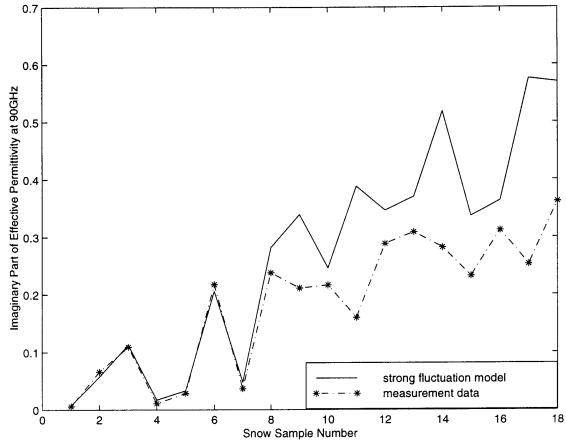

(d)

Figure 7. The imaginary part of effective permittivity of 18 snow samples at (c) 60 *GHz*, and (d) 90 *GHz*. Note that the imaginary part of effective permittivity is a function of mean radius of ice particles, dry snow density and temperature of snow samples. These characteristics of the employed 18 snow samples are given in Table 1.

mittivity in the 1- to 100-GHz range except for large grain sizes at high frequencies $(60 \sim 90\ GHz)$. Other models for the imaginary part of effective permittivity are restricted within low frequencies.

REFERENCES

1. Hallikainen, M., F. Ulaby, and M. Abdelrazik, "Dielectric properties of snow in 3 to 37 GHz range," *IEEE Trans. on Antennas and Propagation,* Vol. 34, No. 11, 1329–1340, 1986.
2. Mätzler, C., "Application of the interaction of microwave with natural snow cover," *Remote Sensing Reviews,* No. 2, 259–387, 1987.
3. Tiuri, M. E., A. Sihvola, E. G. Nyfors, and M. T. Hallikainen, "The complex dielectric constant of snow at microwave frequencies," *IEEE J. Oceanic Eng.,* Vol. 9, 377–382, 1984.
4. Tsang, L., J. A. Kong, and R. W. Newton, "Application of strong fluctuation random medium theory to scattering of electromagnetic waves from a half-space of dielectric mixture," *IEEE Trans. on Antennas and Propagation,* Vol. 30, No. 2, 292–302, 1982.
5. Stogryn, A., "The bilocal approximation for the effective dielectric constant of an isotropic random medium," *IEEE Trans. on Antennas and Propagation,* Vol. 32, No. 5, 517–520, 1984.
6. Tsang, L., and J. A. Kong, "Scattering of electromagnetic waves for random media with strong permittivity fluctuations," *Radio Sci.,* Vol. 16, 303–320, 1981.
7. Nghiem, S. V., R. Kwok, J. A. Kong, and R. T. Shin, "A model with ellipsoidal scatters for polarimetric remote sensing of an isotropic layered media," *Radio Sci.,* Vol. 28, 687–703, 1993.
8. Nghiem, S. V., R. Kwok, S. H. Yueh, J. A. Kong, C. C. Hsu, M. A. Tassoudji, and R. T. Shin, "Polarimetric scattering from layered media with multiple species of scatters," *Radio Sci.,* Vol. 30, 835–852, 1995.
9. Nghiem, S. V., R. Kwok, J. A. Kong, R. T. Shin, S. A. Arcone, and A. J. Gow, "An electrothermodynamic model with distributed properties for effective permittivity of sea ice," *Radio Sci.,* Vol. 31, 297–311, 1996.
10. Hallikainen, M., F. Ulaby, and T. Deventer, "Extinction behavior of dry snow in the 18- to 90-GHz range," *IEEE Trans. Geosci. Remote Sensing,* Vol. 25, No. 6, 737–745, 1987.
11. Mätzler, C., and U. Wegmüller, "Dielectric properties of freshwater ice at microwave frequencies," *J. Phys. D: Appl. Phys. 20,* 1623–1630, 1987.

12. Squeira, P. R., and K. Sarabandi, "Determination of effective permittivity for three-dimensional random media," *1996 IEEE Antenna & Propagation International Symposium,* Vol. 3, 1780–1783, 1996.
13. Sarabandi K., E. S. Li, and A. Nashashibi, "Modeling and measurements of scattering from road surface at millimeter-wave frequencies," *IEEE Trans. on Antennas and Propagation,* Vol. 45, No. 11, 1679–1688, 1997.
14. Ulaby, F., R. Moore, A. Fung, *Microwave Remote Sensing,* Vol. III, Artech House, Inc., Norwood, 1986.
15. Hufford, G., "A model for the complex permittivity of ice at frequencies below 1THz," *Int. J. IR and MM Waves,* Vol. 12, No. 7, 677–682,1991.
16. Mätzler C., "Autocorrelation functions of granular media with free arrangement of spheres, spherical shells or ellipsoids," *J. Applied Physics,* Vol. 81, 1509–1517, 1997.